JCB Article

Integrin-linked kinase is required for laminin-2–induced oligodendrocyte cell spreading and CNS myelination

Soo Jin Chun,[1] Matthew N. Rasband,[2] Richard L. Sidman,[1] Amyn A. Habib,[1] and Timothy Vartanian[1]

[1]Department of Neurology, Beth Israel Deaconess Medical Center, Center for Neurodegeneration and Repair and the Program in Neuroscience, Harvard Medical School, Boston, MA 02115
[2]Department of Neuroscience, University of Connecticut Health Center, Farmington, CT 06030

Early steps in myelination in the central nervous system (CNS) include a specialized and extreme form of cell spreading in which oligodendrocytes extend large lamellae that spiral around axons to form myelin. Recent studies have demonstrated that laminin-2 (LN-2; α2β1γ1) stimulates oligodendrocytes to extend elaborate membrane sheets in vitro (cell spreading), mediated by integrin α6β1. Although a congenital LN-2 deficiency in humans is associated with CNS white matter changes, LN-2–deficient (*dy/dy*) mice have shown abnormalities primarily within the peripheral nervous system. Here, we demonstrate a critical role for LN-2 in CNS myelination by showing that *dy/dy* mice have quantitative and morphologic defects in CNS myelin. We have defined the molecular pathway through which LN-2 signals oligodendrocyte cell spreading by demonstrating requirements for phosphoinositide 3-kinase activity and integrin-linked kinase (ILK). Interaction of oligodendrocytes with LN-2 stimulates ILK activity. A dominant negative ILK inhibits LN-2–induced myelinlike membrane formation. A critical component of the myelination signaling cascade includes LN-2 and integrin signals through ILK.

Introduction

Formation of myelin is a function of oligodendrocytes in the central nervous system (CNS) and Schwann cells in the peripheral nervous system (PNS) in subtle interaction with adjacent axons. To decipher the molecular mechanisms involved in this process in the CNS, we have reduced myelination to three fundamental but likely interrelated cell biological mechanisms: (1) a "cell spreading" machinery to form the large surface membrane characteristic of differentiated oligodendrocytes; (2) specific cell-cell recognition molecules that stabilize oligodendrocyte–axon interactions; and (3) a molecular motor that drives spiraling of the oligodendrocyte's leading edge around the axon.

Here, we have focused on cell spreading, which involves the elaboration of large membrane sheets, and on the genesis of specialized sites on the cell surface for contact with axons. Clues to the molecular mechanisms involved have come from previous studies, which showed that laminin-2 (LN-2; α2β1γ1), also called merosin, promotes extensive membrane production by oligodendrocytes through integrin α6β1 in vitro (Buttery and ffrench-Constant, 1999). Importantly, LN-2 is expressed on the axonal surface in the developing CNS (Colognato et al., 2002), whereas in the developing PNS, it is expressed in the basal lamina. Furthermore, in the PNS, integrin β1–null Schwann cells migrate, proliferate and survive, but have a defect in the ensheathment of axons and formation of myelin (Feltri et al., 2002). These results prompted us to ask whether LN-2 and integrin β1 might also be important for cell spreading and myelination by CNS oligodendrocytes.

Consistent with the studies described above, congenital LN-2 deficiency in humans is associated with CNS white matter changes as shown by magnetic resonance imaging (Farina et al., 1998). However, LN-2–deficient (*Lama2*^{dy}) mice (formerly symbolized as *dy*, dystrophia muscularis, or *mer*, merosin; we refer to the affected homozygotes hereafter as, *dy/dy*) have been reported to exhibit primarily a neuro-

Address correspondence to Timothy Vartanian, Dept. of Neurology, Beth Israel Deaconess Medical Center, Center for Neurodegeneration and Repair and the Program in Neuroscience, Harvard Medical School, 77 Ave. Louis Pasteur, Boston, MA 02115. Tel.: (617) 667-0805. Fax: (617) 667-0836. email: tvartani@caregroup.harvard.edu

Key words: *dy/dy* mice; LN-2; ILK; PI3K; focal adhesion

Abbreviations used in this paper: CC, corpus callosum; CNS, central nervous system; DN, dominant negative; FA, focal adhesion; H&E, hematoxylin and eosin; ILK, integrin-linked kinase; LN-2, laminin-2; MBP, myelin basic protein; MOI, multiplicity of infection; O1, mAb to galactocerebroside; ON, optic nerve; OPC, oligodendrocyte precursor cell; P, postnatal; PI3K, phosphoinositide 3-kinase; PLO, poly-L-ornithine; PNS, peripheral nervous system; SC, spinal cord; SN, sciatic nerve; TN-C, tenascin-C; TRE, tetracycline responsive promoter; TSP-1, thrombospondin-1.

muscular phenotype including peripheral nerve hypomyelination and dysmyelination, with little evidence of defects in CNS myelination (Tsuji and Matsushita, 1985; Matsumura et al., 1997). The β1 integrin signal can function through integrin-linked kinase (ILK), a 59-kD multidomain focal adhesion (FA) protein, which functions as a molecular scaffold at cell-ECM adhesion sites and participates in signal transduction pathways that control cell survival, differentiation, morphology, proliferation, and gene expression in mammalian cells (Wu and Dedhar, 2001). Within FA complexes, ILK can interact with other FA proteins such as paxillin, affixin, and CH-ILKBP (Tu et al., 2001). In *Caenorhabditis elegans* and *Drosophila melanogaster*, loss of function mutations in ILK and integrin-null mutations result in comparable phenotypes (Zervas et al., 2001; Mackinnon et al., 2002). The activation of ILK is phosphoinositide 3-kinase (PI3K) dependent, with PI 3,4,5-triphosphate, a PI3K lipid product, binding to the pleckstrin homology-like domain of ILK and activating its serine/threonine kinase activity (Dedhar, 2000).

Here, we have further defined the phenotype of *dy/dy* mice by identifying hypomyelination in small-diameter axons and dysmyelination in large-diameter axons within the CNS. We have determined the relevant molecular signaling steps for LN-2–induced oligodendrocyte cell spreading and myelin formation in vitro. We show that PI3K activity is required for oligodendrocytes to extend large cytoplasmic sheets, independent of effects on survival, and that ILK is localized within FA complexes of oligodendrocytes and physically associates with other FA proteins such as paxillin. In vivo, ILK is expressed primarily in oligodendrocytes within CNS white matter tracts. Finally, a dominant negative (DN) functioning ILK mutant gene blocks formation of the giant sheets of oligodendrocytes.

We conclude that *dy/dy* mice have defects in CNS myelination, and that the molecular events involved in oligodendrocyte cell spreading and myelin formation include signal transduction cascades using LN-2, integrin β1, PI3K, ILK, and possibly AKT.

Results

dy/dy mice are myelin-deficient and have fewer mature oligodendrocytes

A mutation (*Lama2*^{dy}) in the laminin-α2 chain gene causes of LN-2 deficiency in *dy/dy* mice. These mice show hindleg paralysis at ∼3.5 wk. To test the hypothesis that LN-2 is involved in CNS myelin formation, we first quantified total cell concentration and total mature oligodendrocyte cell concentration in coronal hematoxylin and eosin (H&E)- and CC1-stained sections, respectively, through the corpus callosum (CC; Fig. 1 A). The CC1 antibody recognizes oligodendrocyte cell bodies without labeling myelin (Fuss et al., 2000). We observed a normal concentration of total cells and a 30% reduced concentration of CC1$^+$ oligodendrocytes in the CC of *dy/dy* mice as compared with controls at matched anatomical sites ($P < 0.05$; Fig. 1 B). Despite the normal total cell concentration, the total number of cells was reduced, because the CC area was smaller in the mutants (Fig. 1 A), and the number of mature oligodendrocytes was reduced even more than was indicated by the measured 30% reduction in concentration. The decrease in CC1$^+$ oligodendrocytes was accompanied by a reduction in myelin basic protein (MBP) content on the forebrain determined by immunoblot (Fig. 1 C). In contrast, MBP content in the spinal cord (SC) of *dy/dy* and control mice was equivalent (Fig. 1 C).

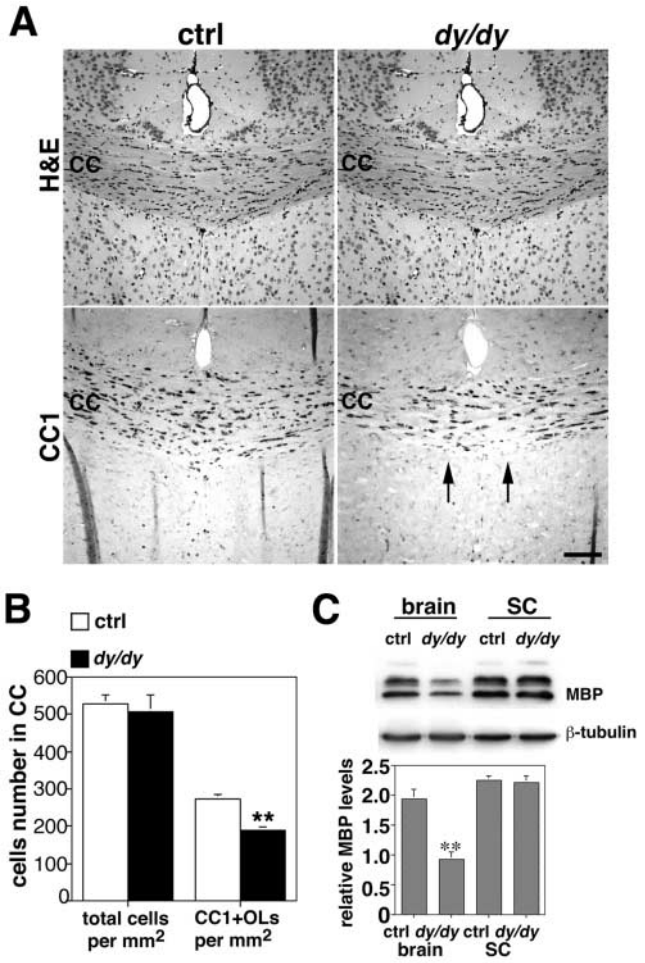

Figure 1. ***dy/dy* mice are myelin-deficient and have fewer mature oligodendrocytes in the CC.** (A) Light micrographs of 6 μm paraffin-embedded coronal sections from 5-wk control (ctrl) and *dy/dy* mice ($n = 3$ of each). A reduction in the CC thickness in *dy/dy* mice is apparent (arrows). Total cells in the CC, a major axonal projection area of the forebrain, were stained by hematoxylin and eosin (H&E; top), and mature oligodendrocytes were immunostained for CC1 (bottom). Bar, 100 μm. (B) The total cell and mature oligodendrocyte numbers in the CC were counted in a grid of constant area at a fixed distance of 0.8 mm from the midline in 10 nonadjacent sections of ctrl and *dy/dy* mice. Although there is no significant difference in total cell concentration, there is a significant reduction in the concentration of CC1$^+$ oligodendrocytes in *dy/dy* CC ($P < 0.05$, asterisks). Because the CC area is smaller in the (A) *dy/dy* mice, the total number of CC1$^+$ cells in the *dy/dy* mice is reduced even >30%. (C) Immunoblot analysis of MBP content was performed in the brain and the SC of ctrl and *dy/dy* mice ($n = 3$). MBP level is significantly reduced in the *dy/dy* brain, but not in SC, compared with controls. Relative MBP levels corrected for loading with β-tubulin are shown ($P < 0.005$, asterisks). Results (B and C) are presented as ±SEM; and comparisons by ANOVA are significant (indicated by asterisks).

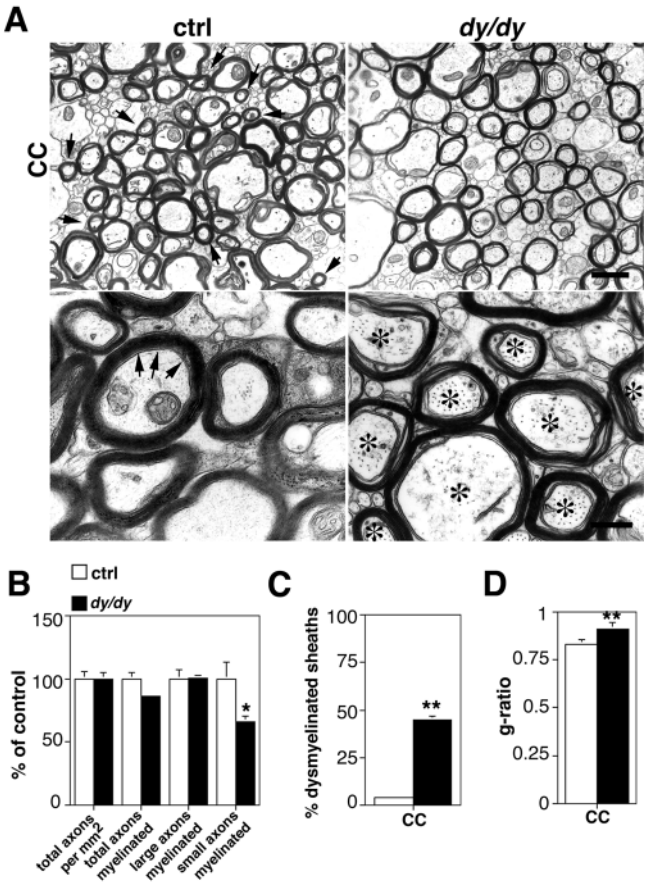

Figure 2. ***dy/dy* mice have dysmyelinated axons in the CC and reduced myelin sheath thickness.** (A) Electron micrographs from the genu of the CC, in midline sagittal sections of ctrl and *dy/dy* mice at 5 wk old ($n = 3$). Axons in the CC are hypomyelinated in *dy/dy* mice (top), and there are fewer small myelinated axons (<0.5 μm, arrows). Bar, 1 μm. Higher magnification (bottom) shows dysmyelination in the majority of *dy/dy* fibers (asterisks), consisting of noncompacted regions in which myelin lamella are separated by pockets of oligodendrocyte cytoplasm, whereas similarly processed controls show well-developed compact myelin (arrows). Bar, 300 nm. (B) Total number of axons, myelinated axons, large axons (axonal diameter; >0.5 μm) and small axons (<0.5 μm) were counted in 20 randomly selected, nonoverlapping fields from mid-sagittal sections through the genu of the CC. The total number of axons per unit area and the number of large and small myelinated axons are presented as percentages of control. The percentage of small myelinated axons is ~30% reduced in *dy/dy* mice ($P < 0.005$, asterisk). (C) The percentage of dysmyelinated myelin sheaths is plotted. Almost 40% of the myelinated axons show noncompacted regions of myelin in *dy/dy* mice ($P < 0.0001$, asterisks), compared with controls. (D) Mean g-ratio (axon diameter/myelinated fiber diameter) was assessed for large axons. The ratio in *dy/dy* mice is substantially different from controls ($P < 0.0001$, asterisks), because even the large axons have abnormally thin myelin sheaths in the mutants. Results (B–D) are presented as ±SEM; and comparisons by ANOVA are significant (indicated by asterisks).

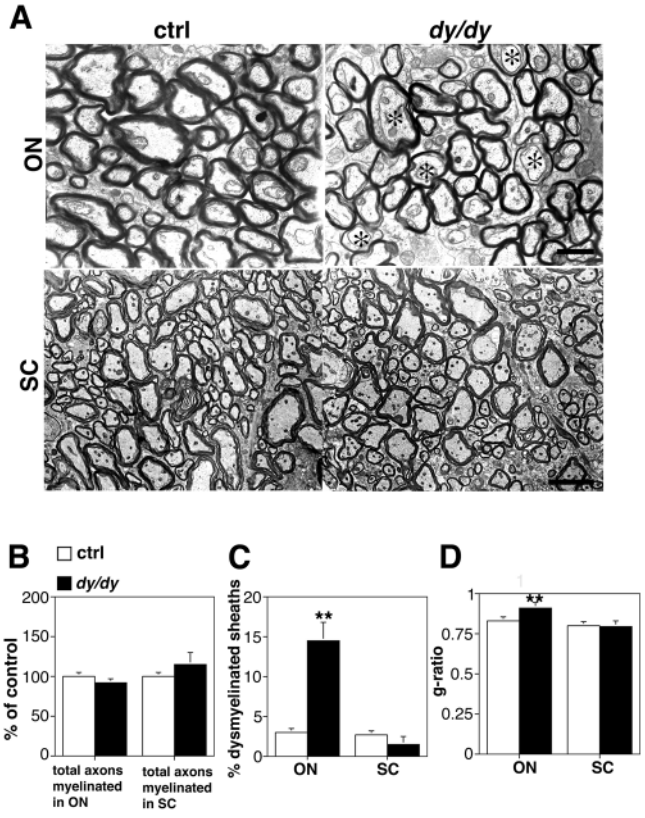

Figure 3. ***dy/dy* mice show dysmyelinated axons also in the ON, but not in the SC.** (A) Electron micrographs of the intracranial portion of the ON and the cervical corticospinal tracts of the SC from 5-wk control and *dy/dy* mice ($n = 3$). The ON in *dy/dy* (top right) contains numerous axons with dysmyelinated sheaths (asterisks), and myelin sheath thickness appears reduced for axons of all calibers. In contrast, the compactness and thickness of myelin lamellae appear indistinguishable from normal in the SP of *dy/dy* mice (bottom). Bars: (top) 1 μm; (bottom) 4 μm. (B) The concentration of myelinated axons was counted in 20 randomly selected, nonoverlapping fields from sections through the ON and SC. The total number of axons per unit area in *dy/dy* mice is expressed as percentages of the controls (ctrl). There are no differences in myelinated axon concentration in the ON or SC of ctrl and *dy/dy* mice. Results are presented as ±SEM; and ANOVA revealed no statistical differences. (C) Percentages of dysmyelinated sheaths are shown. The ON of *dy/dy* mice contain ~15% dysmyelinated axons, a significant increase over the controls ($P < 0.05$, asterisks). No significant dysmyelination is observed in the SC of *dy/dy* mice. (D) Mean g-ratio in *dy/dy* mice is significantly different from controls ($P < 0.001$, asterisks). No decrease is observed in the abundance of myelin sheaths and no morphological deficits are found in the SC of *dy/dy* mice. Results (C and D) are presented ±SEM; and comparisons by ANOVA are significant (indicated by asterisks).

Ultrastructural analysis of *dy/dy* mice: regional differences

The above results suggest a defect in forebrain myelination in *dy/dy* mice. To determine whether myelin structure as well as myelin content is compromised, we analyzed by EM sagittal sections of CC (Fig. 2), transverse sections of optic nerve (ON; Fig. 3), and corticospinal tract in transverse sections of cervical SC (Fig. 3). In the CC, we divided myelinated axons into large diameter (axons > 0.5 μm), and small diameter (axons < 0.5 μm) groups and observed ~30% reduction in the number of small diameter axons per unit area that were myelinated in *dy/dy* mice ($P < 0.005$; Fig. 2, A and B). The total number of axons per unit area was not changed (Table I). Higher magnification revealed that ~40% of myelinated axons in *dy/dy* mice showed ultrastructural abnormalities ($P < 0.0001$) with large pockets of oligodendrocyte cyto-

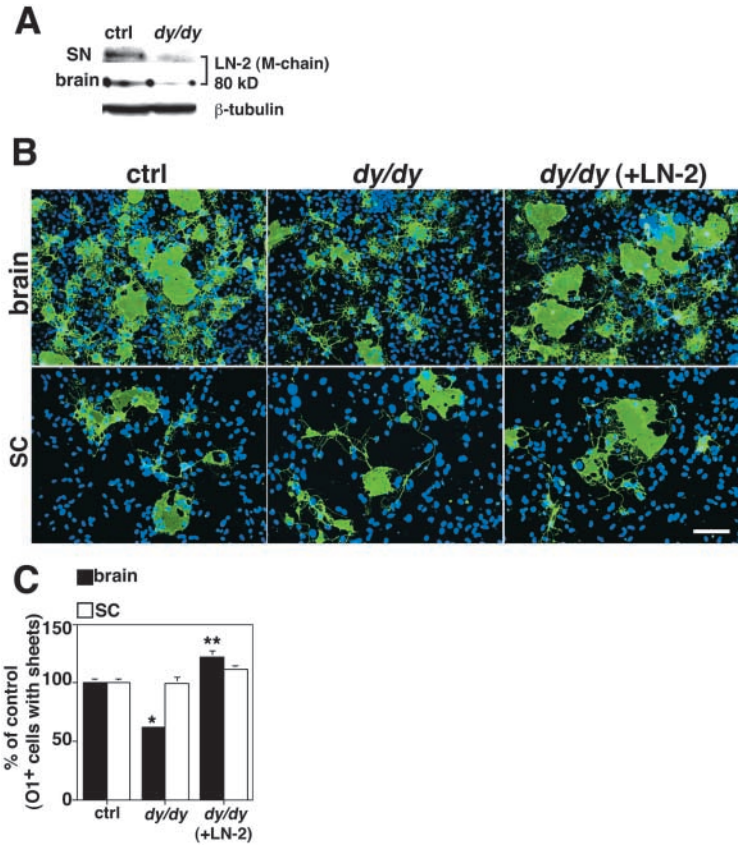

Figure 4. **Oligodendrocytes from *dy/dy* brain (CC) are more responsive to LN-2 than those from the *dy/dy* SC.** (A) Levels of LN-2 (M-chain, 80kD) were detected by immunoblot. The lysates were prepared from the SN and 10 d-mixed glial cell cultures from the CC area of brain and from the SC of P day 1 pups. The *dy/dy* mice show no LN-2 expression in the SN and reduced levels in the brain, compared with controls ($n = 3$). β-Tubulin levels were detected as a control. (B) The mixed glial cells from the brain and SC were cultured in 2% FBS for 10 d on poly-L-ornithine (PLO) or LN-2 and stained for O1 (green), as a marker for maturing oligodendrocytes, and DAPI (blue) for nuclei. Bar, 100 μm. 10 and 5% of cells from the brain and the SC showed $O1^+$, respectively. The *dy/dy* cells on PLO generally failed to show cell spreading, in dramatic contrast to those cultured on LN-2. (C) The relative percentages of $O1^+$ cells with broad myelin membrane sheets were counted. In confirmation of the image data in B, $O1^+$ cells prepared from *dy/dy* brain on LN-2 showed dramatically increased oligodendrocyte cell spreading compared with those on PLO ($P < 0.0001$, asterisk) or compared with $O1^+$ cells from control brain on PLO ($P < 0.05$, asterisks). Although $O1^+$ cells prepared from the SC of *dy/dy* mice showed an increase on LN-2 than on PLO or control, the difference was not significant. Results are presented as ±SEM; and comparisons by ANOVA are significant (indicated by asterisks).

plasm separating myelin lamellae (Fig. 2, A and C). Mean myelin sheath thickness in *dy/dy* mice was ~0.04 μm compared with the thickness of ~0.09 μm in controls ($P < 0.0001$). The average diameter of axons in control and *dy/dy* mice did not differ significantly; the difference in mean g-ratio (axonal diameter/total fiber diameter) of 0.82 for control fibers versus 0.91 in *dy/dy* mice ($P < 0.0001$; Fig. 2 D) indicates myelin reduction in the mutants.

In the ON from *dy/dy* mice, ~15% of the axons were dysmyelinated compared with none in controls ($P < 0.05$; Fig. 3, A and C). The total cross-sectional area of the nerve and the number of myelinated axons per unit area were not changed (Fig. 3 B), but the g-ratio was significantly increased compared with controls ($P < 0.001$; Fig. 3 D), to the same extent as in the CC. In the SC, consistent with the levels of MBP staining by immunoblot (Fig. 1 C), the total number of myelinated axons (Fig. 3 B), myelin morphology (Fig. 3 C) and myelin thickness (not depicted) were normal. These results highlight the regional differences in myelination in *dy/dy* mice.

Table I. **Concentration of small diameter myelinated axons is decreased in *dy/dy* mice**

	Total axons/mm^2	Myelinated axons		Unmyelinated axons	
		[L]	[S]	[L]	[S]
ctrl	228 ± 12.4	40 ± 2.8	25 ± 3.3	15 ± 1.4	147 ± 11.4
dy/dy	228 ± 11.1	40 ± 1.2	17 ± 1.1	15 ± 0.7	156 ± 10.6

The number of large and small diameter axons that are myelinated and unmyelinated (total axons) per unit area (mm^2) in the control and in the *dy/dy* mice was counted. *t* test revealed a statistically significant reduction of small myelinated axons in *dy/dy* mice ($P < 0.05$). [L] = large diameter axons (>0.5 μm); and [S] = small diameter axons (< 0.5 μm).

Responsiveness of oligodendrocytes to LN-2 in *dy/dy* mice: regional differences

Given the regional specificity of myelination abnormalities in *dy/dy* mice, we next explored whether oligodendrocytes from different regions of these mice show different behavior on LN-2 in vitro. Although the mutation in *dy/dy* mice has not yet been identified, these mice express small amounts of apparently normal LN-2 in muscle, but no LN-2 in peripheral nerves (Guo et al., 2003). We cultured mixed glial cell preparations from the CC region of the forebrain and from the SC of postnatal (P) day 1 pups for 10 d and labeled cells with mAb to galactocerebroside (O1).

10 and 5% of cells from the brain and the SC, respectively, showed O1 immunoreactivity. The *dy/dy* pups were distinguished from +/+ and +/*dy* littermates in immunoblots by showing markedly reduced levels of LN-2 (M-chain) in the sciatic nerve (SN) and mixed glial cultures of the brain, respectively, compared with controls (Fig. 4 A). The *dy/dy* cells on poly-L-ornithine (PLO) generally failed to show cell spreading, in dramatic contrast to those cultured on LN-2 (Fig. 4. B). $O1^+$ cells prepared from *dy/dy* brain on LN-2 showed dramatically increased oligodendrocyte cell spreading compared with those on PLO ($P < 0.0001$) or compared with $O1^+$ cells from control brain on PLO ($P < 0.05$; Fig. 4 C). Although $O1^+$ cells prepared from the SC of *dy/dy* mice showed larger processes on LN-2 than on PLO or

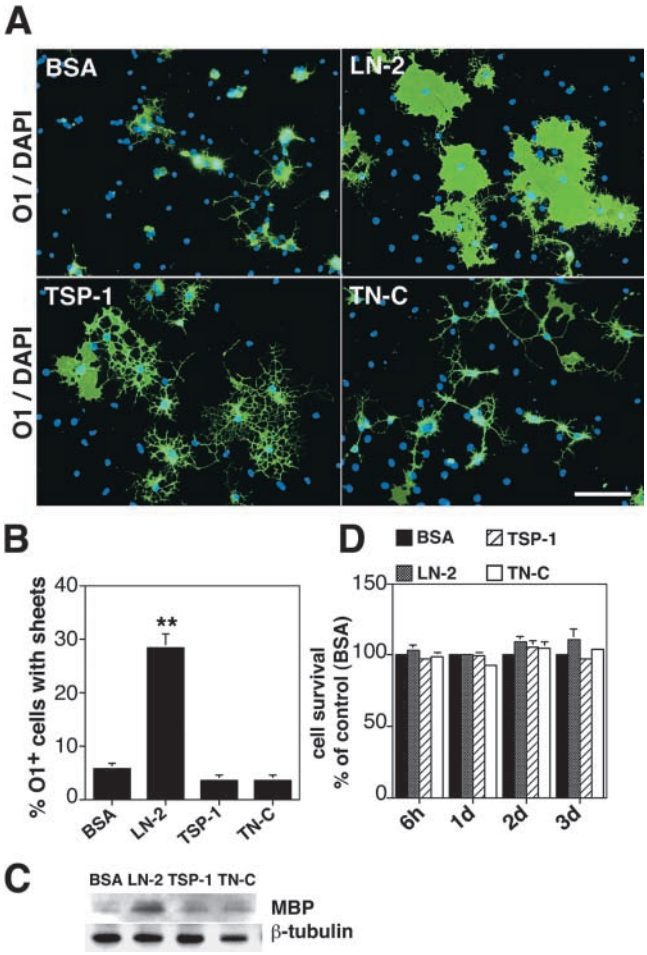

Figure 5. **LN-2 promotes oligodendrocyte cell spreading in vitro.** (A) Purified OPCs isolated from the rat forebrain were cultured in the presence of PDGF and basic FGF for 3 d. Cells were fixed after three further days of growth on BSA, LN-2, TSP-1, and TN-C in serum-free media with N_2 supplement (N_2). Cells were plated and stained for O1 (left, green) and DAPI (blue). Bar, 100 μm. (B) The relative percentages of $O1^+$ cells with broad myelin membrane sheets on different ECM substrates were scored. LN-2 increases the ratio of $O1^+$ cells with myelin membrane sheets to the total number of $O1^+$ cells. Results are presented as ±SEM; and comparisons by ANOVA are significant at $P < 0.0001$ (indicated by asterisks). Average diameter of $O1^+$ cells with sheets is 140 ± 20 μm in the LN-2–treated cells, compared with 90 ± 15 μm in the other ECMs-treated cells. (C) MBP levels were detected by immunoblot. The cell lysates were prepared 3 d after plating on ECMs. The MBP level on LN-2, but not on other ECMs, is increased. (D) The effects of ECMs on cell survival for 3 d were measured by the Alamar blue assay. Cells were plated on the various ECMs and incubated for 6 h, 1 d, 2 d, or 3 d. Results are presented as ±SEM; and ANOVA revealed no statistical differences in survival between the substrates.

a control (Fig. 4 B), the difference was not significant (Fig. 4 C). These data show that oligodendrocytes from the brain surrounding the CC were more responsive to LN-2 than those from the SC.

LN-2 enhances myelin membrane formation in oligodendrocytes in vitro

To define the molecular mechanisms through which LN-2 may regulate myelination, we used the culture paradigm of Buttery and ffrench-Constant (1999) in which ECM components influence oligodendrocyte morphology. We plated oligodendrocyte precursor cells (OPCs) on four different types of ECM and labeled with oligodendrocyte-specific antibodies to O1 and MBP.

O11 cells grown on LN-2 extended broad sheetlike processes in contrast to cells on BSA, thrombospondin-1 (TSP-1), or tenascin-C (TN-C; Fig. 5 A), and the difference was highly significant ($P < 0.0001$; Fig. 5 B). Average $O1^+$ cell diameter with sheets was 140 μm ± 10 in the LN-2–treated cells compared with 90 μm ± 15 in the other ECMs-treated cells. In addition, LN-2 enhanced the percentage of MBP^+ cells ($P < 0.0001$) and increased the MBP levels detected by immunoblot (Fig. 5 C; unpublished data). The increase in number of $O1^+$ cells bearing sheets was not due to increased cell survival on LN-2. Cells were plated on different ECMs for 6 h, 1 d, 2 d and 3 d and cell survival was measured through the Live/Dead Cytotoxicity and the Alamar blue assays. Both assays indicated no statistical differences in survival between the substrates (Fig. 5 D).

LN-2 promotes oligodendrocyte cell spreading through PI3K, but not MAPK

Because PI3K is involved in integrin β1–mediated cell spreading in various cell types, we hypothesized that LN-2 may enhance oligodendrocyte cell spreading through PI3K. PI3K activity was determined by measuring activation of AKT, a primary downstream substrate of PI3K. OPCs were replated on different ECMs, and 45 min and 6 h later the level of phosphorylation was determined by immunoblot with a phospho-AKT ser473 antibody (Fig. 6 A). LN-2, TSP-1, and TN-C all activated the phosphorylation of AKT at 45 min. However, LN-2 activated AKT phosphorylation continuously up to 6 h in contrast to other ECMs, suggesting that AKT phosphorylation might be important for LN-2–induced cell spreading in oligodendrocytes.

Because LN-2 promotes membrane production through integrin α6β1 and both PI3K and MAPK pathways are activated by integrin α6β1, we sought possible involvement of these two molecular pathways in the effects of LN-2 on oligodendrocytes in vitro. These pathways were disrupted with small molecule inhibitors: 0.01 μM wortmannin (irreversible PI3K inhibitor); 0.5 μM LY294002 (reversible PI3K inhibitor); and 4 μM U0126 (MAPK/ERK inhibitor). These inhibitors blocked the phosphorylation of AKT and MAPK in a time-dependent manner (Fig. 6, B–D). Inhibitors of PI3K but not MAPK pathways disrupted LN-2–enhanced membrane sheet formation (Fig. 6 E). 30% of $O1^+$ cells on LN-2 formed broad myelin membrane sheets (Fig. 6 G). However, the inhibitors of PI3K blocked formation of these sheetlike processes; >50% of cells with long processes lacked membrane sheets ($P < 0.005$). We found no influence of MAPK inhibitor on LN-2–induced cell spreading (Fig. 6, E and G). Together, these results suggest that LN-2 promotes oligodendrocyte cell spreading through the PI3K but not the MAPK pathway.

Because AKT is one of crucial downstream effectors of PI3K, we examined the functional role of AKT in LN-2–induced oligodendrocyte cell spreading by using a DN-

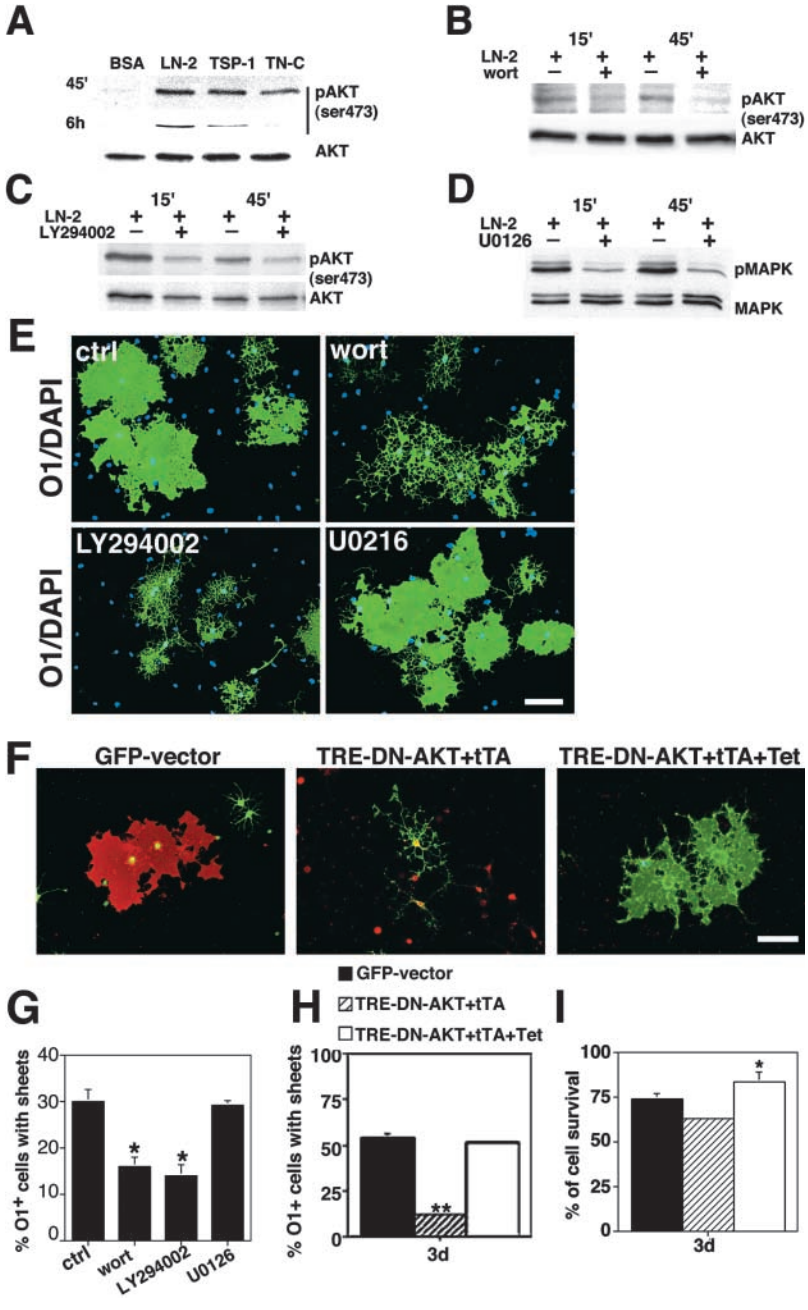

Figure 6. **Oligodendrocyte cell spreading promoted by LN-2 requires PI3K, not MAPK.** (A) 45 min and 6 h after cells were plated on BSA, LN-2, TSP-1 and TN-C, phosphorylation of AKT was detected by immunoblot with AKT phospho-ser473 (pAKT) antibody. AKT levels were detected as controls. (B–D) The blocking effects of both 0.01 μM wortmannin (wort) and 0.5 μM LY294002 (PI3K inhibitors) on pAKT or of 4 μM U0126 (MAPK/ERK inhibitor) on pMAPK at 15 and 45 min were shown by immunoblot. AKT or MAPK levels were detected as controls. (E) Cells were fixed after 3 d growth on LN-2 with various inhibitors at the same concentrations used in B–D, after pretreatment for 5 min before plating and staining by O1 (green) and DAPI (blue). Bar, 100 μm. (F) OPCs were plated on LN-2 and infected with GFP-vector (20 MOI) alone or a DN-AKT (10 MOI) in serum-free media with N_2 for 3 d by an adenovirus-mediated tetracycline (Tet)–off inducible system. Double staining with O1 (left, red) and GFP (left, green) or with O1 (middle and right, green) and HA-epitope–tagged DN-AKT (middle and right, red) delineates cells infected by vector or DN-AKT. Incubation of tetracycline responsive promoter (TRE)-DN-AKT (10 MOI) with tetracycline-controlled transactivator (tTA, 10 MOI) blocks LN-2–induced cell spreading by expression of DN-AKT. Incubation with 10 μg/ml Tet turned off the expression of DN-AKT, showing cell spreading as much as GFP-vector alone. Bar, 100 μm. (G) The relative percentage of $O1^+$ cells with broad myelin membrane sheets on LN-2 with various inhibitors is shown. Treatment with PI3K inhibitors reduces myelin membrane formation up to 50% ($P < 0.005$, asterisks). MAPK inhibitor had no influence on myelin membrane formation. (H) The relative percentage of $O1^+$ cells with broad myelin membrane sheets is shown. Incubation of TRE-DN-AKT (10 MOI) with tTA (10 MOI) decreases cell spreading up to 75% compared with 20 MOI GFP-vector alone ($P < 0.0001$, asterisks). Incubation with 10 μg/ml Tet increases cell spreading up to 50%. (I) Cell survival was measured by the Live/Dead Cytotoxicity assay. There is no statistical difference in cell survival between vector alone (20 MOI) and TRE-DN-AKT (10 MOI) + tTA (10 MOI), whereas addition of Tet increases cell survival ($P < 0.05$, asterisk). Results (G–I) are presented as ±SEM; and comparisons by ANOVA are significant (indicated by asterisks).

AKT (kinase inactive), in which both phosphorylation sites of (Thr308 and Ser473) were replaced by alanine (AA-AKT; Kitamura et al., 1998). HA-epitope–tagged DN-AKT was expressed in the cells after incubation with tetracycline responsive promoter (TRE)-DN-AKT and tetracycline (Tet)-controlled transactivator (tTA) for 3 d by adenovirus-mediated Tet–off inducible system. Although GFP vector alone (20 multiplicity of infection [MOI])-transfected $O1^+$ cells on LN-2 formed 50% broad sheetlike processes consistent with myelin membrane sheets in 3 d (Fig. 6, F and H), TRE-DN-AKT(10 MOI) and tTA (10 MOI)-transfected cells decreased LN-2 induced cell spreading by nearly 75% (Fig. 6, F and H; $P < 0.0001$). However, additional incubation with 10 μg/ml Tet turned off the expression of DN-AKT, showing as much cell spreading as with GFP-vector alone (Fig. 6, F and H). Furthermore, there was no statistically significant difference on cell survival between GFP-vector alone– and DN-AKT–transfected cells, but addition of Tet increased cell survival (Fig. 6 I, $P < 0.5$). These results show that AKT activation might be involved in LN-2–enhanced cell spreading in oligodendrocytes.

ILK is localized in oligodendrocytes in vivo and in vitro

Because integrin-linked kinase (ILK), a multidomain FA protein, is critically involved both in the adhesion of cells to the ECM by interacting with integrin β1 and in signal transduction in a PI3K-dependent manner, we hypothesized that ILK is involved in LN-2 signaling of oligodendrocyte cell spreading and myelination. To examine

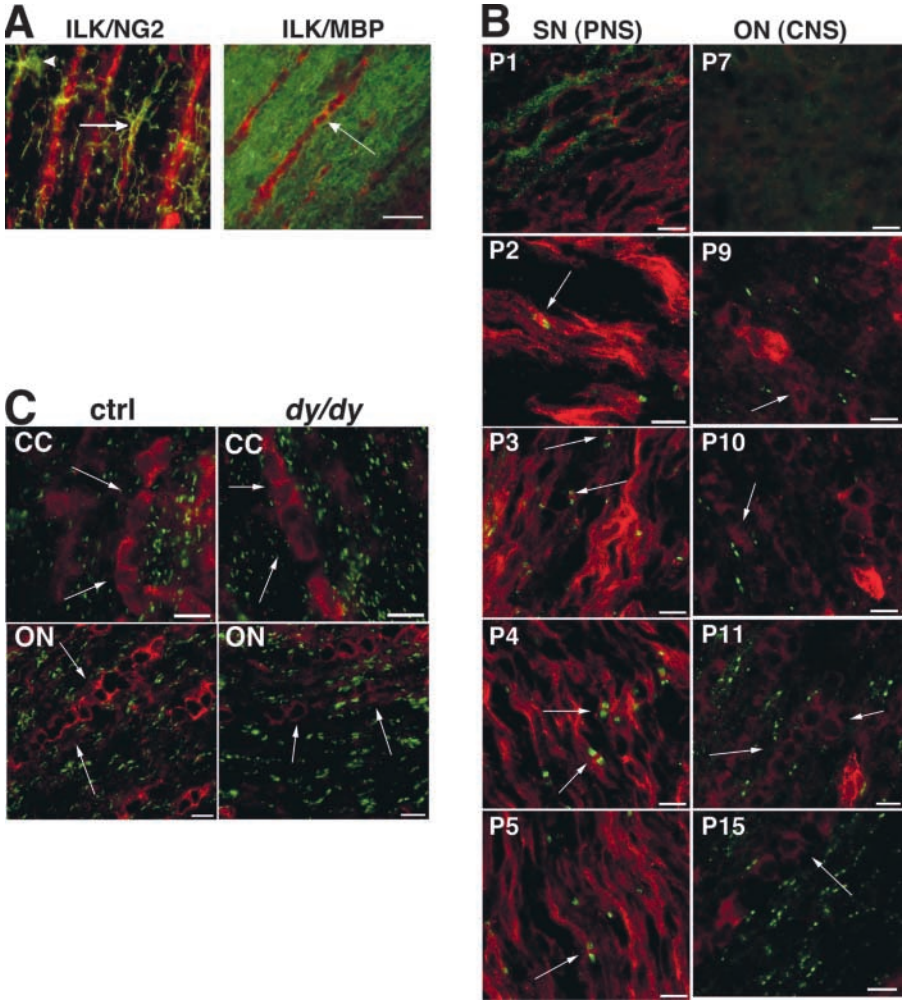

Figure 7. **ILK is expressed in the developing CNS and PNS.** (A) Double staining for ILK (left, red) and NG2 (left, green) or MBP (right, green) in rat CNS ON. Most sites of NG2 immunoreactivity, including cell bodies (arrowhead) are devoid of ILK staining, although occasionally NG2-positive cells are also ILK positive (arrow). In MBP-positive cells, The ILK staining is restricted to long rows of cells residing between fascicles of myelinated axons (arrow). Bar, 10 μm. (B) ILK expression patterns during development of Sprague-Dawley rat SN (left, P days: P1–5) and of rat CNS ON (right, P7, P9–11, and P15). The SN shows localization of ILK (red) to the cytoplasm of Schwann cells at nodes of Ranvier (arrows) throughout the early P developmental phase. In the ON, ILK (red) is restricted to oligodendrocyte cell bodies (arrows), whereas the protein Caspr (green), restricted to paranodal axoglial junctions, serves as a marker of myelination. At P7, myelin has not yet formed, as evidenced by the lack of Caspr staining, and oligodendrocytes do not yet stain for ILK. From P9 onward, both stains are positive. Bars, 10 μm. (C) Double staining with ILK (red) and Caspr (green) in the CC and ON of 5-wk control and *dy/dy* mice. ILK in the CC and the ON of these animals is localized to oligodendrocyte cell bodies. Expression pattern of ILK does not differ significantly between control and *dy/dy* mice, whereas there appears to be a difference in Caspr immunoreactivity, suggesting paranodal abnormalities. Bars, 10 μm.

whether ILK is expressed in oligodendrocytes, we double stained for ILK and NG2 as a marker for OPCs or MBP for mature oligodendrocytes (Fig. 7 A, arrows). Double staining clearly shows that ILK is expressed principally in interfascicular oligodendrocytes.

Next, we investigated ILK expression in vivo during early myelination of rat PNS SN (P days 1–5) and rat CNS ON (P7, P9–11, and P15) and in the CC and the ON of 5-wk control and *dy/dy* mice (Fig. 7 B). ILK was enriched in the rat PNS, specifically in cytoplasmic processes of Schwann cells at nodes of Ranvier. In the rat CNS ON, ILK expression was restricted to interfascicular oligodendrocytes (Fig. 7 B, arrows). Sections double labeled with ILK and Caspr, an axonal component of paranodal axoglial junctions, showed that ILK protein was detected only in oligodendrocytes from P9 onward, when myelination was underway. Double staining with ILK and Caspr in the CC and the ON of 5-wk control and *dy/dy* mice showed that ILK in the adult mouse CNS, as in the developing rat CNS, was localized to oligodendrocyte cell bodies (Fig. 7 C, arrows). There was no significant difference in the ILK expression pattern between control and *dy/dy* mice. These results indicate that ILK is expressed in myelinating cells in rat and mouse PNS and CNS, and may be involved in general in cell spreading in myelinating cells.

ILK shows colocalization with FA proteins such as integrin β1 and paxillin in oligodendrocytes

Given the reported role of ILK in adhesion complexes (Li et al., 1999), we labeled oligodendrocytes for ILK and the FA proteins integrin β1 and paxillin (Fig. 8 A). ILK was localized in the cell body and throughout the processes including their tips, with a high concentration of ILK at the growth cone–like termini. Digitally merged images of differentiating oligodendrocytes on LN-2 demonstrate that ILK colocalizes with integrin β1 in cell bodies and at FA sites in processes (Fig. 8 A, arrows).

Paxillin, a 68-kD FA adaptor molecule involved in integrin signaling, functions in regulation of the actin cytoskeleton (Turner, 2000). Like integrin β1, paxillin colocalized with ILK in FAs (Fig. 8 A). We evaluated the interaction between ILK and paxillin also by coimmunoprecipitation of ILK with paxillin from lysates of cells grown on BSA, LN-2, and in suspension (Fig. 8 B). The results suggest that the ILK–paxillin interaction is constitutive rather than adhesion induced.

LN-2 stimulates ILK activity and DN-ILK blocks LN-2–induced myelin membrane formation

To determine the functional role of ILK in LN-2–induced oligodendrocyte cell spreading, we used a dominant negative ILK

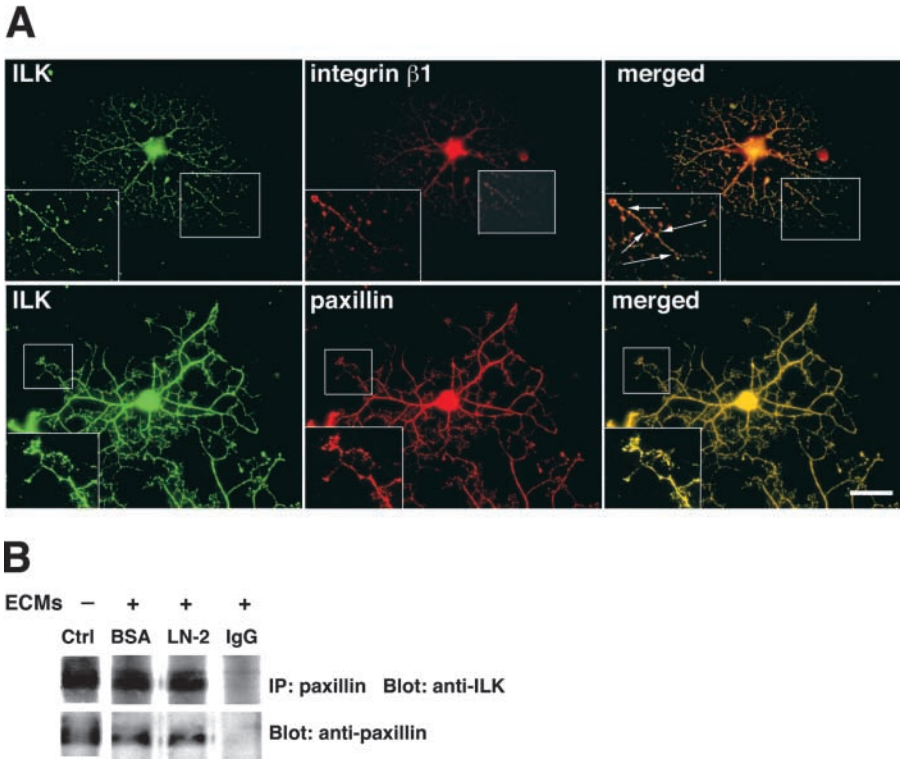

Figure 8. **ILK is expressed in oligodendrocytes in vitro and colocalizes with the FA-associated molecules, integrin β1 and paxillin.** (A) OPCs isolated from P2 Sprague-Dawley rat forebrain were stimulated to differentiate in vitro, and cells were double stained with ILK (green) and integrin β1 (red) or paxillin (red) in differentiated oligodendrocytes plated on LN-2. ILK is distributed throughout the cell body and processes, including the tips of processes (top left) and growth cone–like termini (bottom left) of oligodendrocytes. Higher magnification of merged images (the boxed areas) demonstrates that ILK colocalizes with integrin β1 and paxillin in FAs (arrows). Although integrin β1 is partly colocalized with ILK throughout the cell body and processes, paxillin colocalizes with ILK in every part of the cell. Bar, 30 μm. (B) OPCs were plated and then incubated for 30 min either with ECMs (BSA and LN-2 [with or without IgG]) or without ECMs (Ctrl) and were lysed in NP-40 lysis buffer. Paxillin and control mouse IgG immunoprecipitations were performed and subjected to SDS-PAGE followed by immunoblot with antibodies against ILK. ILK coimmunoprecipitates with the paxillin antibody as compared with the control IgG. Total amounts of lysates were detected by antipaxillin antibody. The results suggest that the ILK–paxillin interaction is constitutive rather than adhesion induced.

loss of function mutation in ILK (DN-ILK; kinase inactive), in which Glu 359 was mutated to Lys (Persad et al., 2000). When GFP-vector or GFP-DN-ILK was inserted into cells by adenovirus-mediated gene transfer, 60% of cells expressed GFP (unpublished data). Transfectants were replated on LN-2 in serum-free media and cultured for 1, 2, or 6 h. ILK activity was determined with exogenous MBP as a substrate. LN-2 induced ILK to phosphorylate MBP in GFP-transfected cells, with a peak at 1 h, but not in cells expressing DN-ILK (Fig. 9 A). Furthermore, LN-2 stimulated ILK activity more effectively than any of the other ECMs at 1 h (Fig. 9 B, $P < 0.5$).

ILK also can phosphorylate PKB/AKT on ser473 directly or indirectly (Delcommenne et al., 1998; Troussard et al., 2003). DN-ILK blocked phosphorylation of AKT ser473 (Fig. 9 C). DN-ILK also inhibited phosphorylation of GSK-3β on ser 9, a downstream substrate of ILK (unpublished data). To test directly whether ILK is involved in LN-2–enhanced oligodendrocyte cell spreading, DN-ILK was expressed in OPCs, which were plated on LN-2 and incubated with vector or DN-ILK (10 or 20 MOI) for 3 d. As a control, we measured cell survival through the Live/Dead Cytotoxicity assay and found no significant cell death in DN-ILK (10 MOI) compared with vector (10 MOI), but, at the higher DN- ILK concentration of 20 MOI, we did find significant cell death (Fig. 9 F).

Staining for O1 and DAPI revealed that 50% of GFP-transfected $O1^+$ cells (10 or 20 MOI) formed broad sheetlike processes consistent with myelin membrane sheets (Fig. 9, D and E). In DN-ILK transfected cells, formation of these sheetlike processes was decreased by nearly 80% ($P < 0.001$). Only 10% of cells transfected with 10 MOI DN-ILK formed membrane sheets, and an even smaller percentage with 20 MOI DN-ILK (Fig. 9, D and E). These results demonstrate that ILK is necessary for LN-2 signaling in oligodendrocyte cell spreading and myelin formation. In summary, LN-2–induced oligodendrocyte cell spreading and myelination in CNS occurs in a PI3K/ILK-dependent manner.

Discussion

LN-2 is required for normal myelination in the CNS

Although congenital LN-2 deficiency in humans leads to CNS white matter changes as detected by magnetic resonance imaging as well as peripheral neuropathy and muscular dystrophy (Morandi et al., 1999), *dy/dy* mice with spontaneously occurring mutations in LN-2 were reported to exhibit phenotypic abnormalities limited to PNS myelination and skeletal muscle (Bradley and Jaros, 1979), except for the report of CNS myelin abnormalities in mice by Tsuji and Matsushita (1985). Here, we analyzed 5-wk-old *dy/dy* and littermate control mice for possible involvement of this gene in CNS myelination. In the CC of *dy/dy* mice, we found (1) reduced thickness of the CC; (2) a 30% reduction in the concentration of mature oligodendrocytes without a

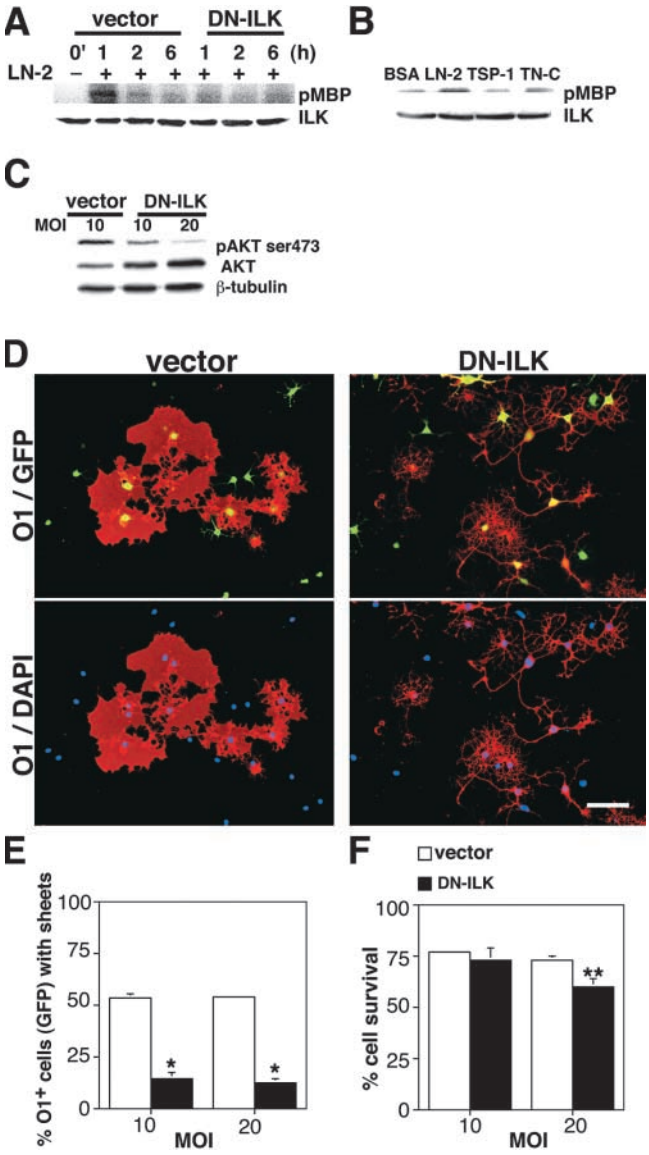

Figure 9. **LN-2 activates ILK activity and DN-ILK inhibits oligodendrocyte cell spreading.** (A) OPCs were transfected with 10 MOI vector alone as a control or with DN-ILK (kinase-inactive form of ILK) by adenovirus gene transfer. After 24 h, transfectants were plated on LN-2 in serum-free media with N_2 and cultured for the indicated time periods. ILK was immunoprecipitated from cell extracts. ILK activity was determined with MBP as an exogenous substrate. Total amounts of ILK proteins in the immunoprecipitates were detected by immunoblot with an anti-ILK antibody. Results indicate that LN-2 stimulates ILK activity. (B) 1 h after cells were plated on BSA, LN-2, TSP-1, and TN-C. ILK activity was detected by phosphorylation of MBP. ILK levels were detected as controls. LN-2 stimulates ILK activity more effectively than any of the other ECMs at 1h ($P < 0.5$) (C) The blocking effect of DN-ILK on pAKT ser473 was investigated by immunoblot. Cells were plated on LN-2 and incubated with 10 MOI vector or 10 or 20 MOI DN-ILK for 3 d. Compared with vector, DN-ILK blocks phosphorylation of AKT ser473. AKT and β-tubulin serve as standards for the total amount of protein. (D) OPCs were plated on LN-2 and incubated with 10 or 20 MOI GFP-vector or GFP-DN-ILK in serum-free media with N_2 for 3 d. Cells were fixed and stained for O1 (red) and with DAPI for nuclei (blue). Double staining with O1 and GFP (top) or with O1 and DAPI (bottom) delineates cells infected by vector or DN-ILK. DN-ILK blocks LN-2–induced cell spreading. Bar, 100 μm. (E) The relative percentage of GFP-expressing $O1^+$ cells with broad myelin membrane sheets is shown. 20 MOI DN-ILK decreases cell spreading up to 75% compared with vector alone ($P < 0.005$, asterisks). (F) Cell survival was measured by the Live/Dead Cytotoxicity assay. There is no statistical difference in cell survival between 10 MOI vector and 10 MOI DN-ILK, whereas 20 MOI DN-ILK induces cell death ($P < 0.01$, asterisks). (E and F) Results are presented as ±SEM; and comparisons by ANOVA are significant (indicated by asterisks).

change in total glial cell concentration; and (3) defects in myelin lamellar compaction and sheath thickness. These results agree with previous studies (Buttery and ffrench-Constant, 1999) showing that LN-2 promotes formation of myelin membrane in vitro and further suggest that *dy/dy* mice may show developmental defects expressed as a disturbance in lamellar organization or oligodendrocyte cell volume. However, these results may also reflect a decrease in oligodendrocyte survival.

Small-sized axons are preferentially affected

Hypomyelination is particularly evident in small-sized axons. We found an ~30% reduction in the concentration of small-sized (<0.5 μm) axons that were myelinated in *dy/dy* CC, whereas the total number of myelinated axons in the same area was not changed. The preferential reduction in myelination of small-sized axons may reflect an inability of individual oligodendrocytes to extend multiple cytoplasmic processes and envelope a cluster of small- sized axons, without a corresponding defect in their ability to wrap around large-sized axons (Bjartmar et al., 1994). Oligodendrocyte cell bodies might lie closely associated with large-sized axons, without a requirement to reach them by extending cytoplasmic processes (Hildebrand et al., 1993). Accordingly, impaired formation of oligodendrocyte processes and membrane sheets would cause a more pronounced hypomyelination in tracts rich in small-sized axons than in tracts with large-sized axons. Another possible explanation for the differences between the abnormalities in small- and large-sized axons is that myelination may be delayed in the CNS of *dy/dy* mice, as it is in the PNS, because large-sized axons are generally myelinated earlier than small-sized axons in the CNS (Schwab and Schnell, 1989).

Regional differences

The dramatic differences between PNS and CNS myelination in the spontaneous *dy/dy* mutant mouse, described by several investigators approximately three decades ago (Bradley and Jaros, 1979), merit reconsideration. In segments of nerve roots of almost all cranial nerves and segments of both dorsal and ventral roots of cervical, lumbar, and sacral spinal nerves examined by EM, large clusters of small diameter axons are completely unmyelinated and lie contiguous with one another, without intervening Schwann cell cytoplasmic strands. Given that the gene product, LN-2, is a surface membrane constituent of axons, it now seems clear that the myelination problem at these restricted sites results not from a deficient number of Schwann cells caused by reduced cell division or excessive cell death, but from a failure of myelinating cells in the PNS and CNS to respond to the β1 component of LN-2 via PI3K and ILK by extending cytoplasmic

sheets, which are to envelop axons and form myelin lamellae. An unresolved problem is why myelination in the PNS is essentially normal in the few millimeters of the nerve roots closest to the SC, as well as throughout nerves distal to the roots, but grossly abnormal in relatively short intervening segments of the roots. This is a general problem with neurological genetic diseases, which commonly show a remarkable selectivity within what we generally assume to be a uniform population of target cells.

Here, we found regional differences in myelination and oligodendrocyte cell spreading within the CNS: (1) SC corticospinal tracts exhibited no reduction in myelin content and no dysmyelination, in contrast to the ON and CC, which were hypomyelinated and showed many dysmyelinated axons; and (2) Oligodendrocytes of the SC are less responsive to LN-2 than those of the CC. These data suggest that LN-2 might be a crucial factor for myelination only in selected areas of the CNS. Interestingly, *Fyn*-knockout mice exhibit a pattern of regional differences within the CNS similar to what we have found in *dy/dy* mice (Sperber et al., 2001).

LN-2 signaling in oligodendrocyte cell spreading is PI3K dependent

We observed that LN-2, TSP-1, and TN-C all activated the phosphorylation of AKT at 45 min. However, for the antiadhesive proteins, TSP-1 and TN-C, PI3K and AKT activation is transient. LN-2 activated AKT phosphorylation continuously for up to 6 h, suggesting that sustained AKT phosphorylation might be important for LN-2–induced cell spreading in oligodendrocytes. A role for AKT phosphorylation is also supported by our data that DN-AKT expression in an adenovirus-mediated Tet–off inducible system decreased LN-2–induced cell spreading. However, longer-term AKT activation remains to be examined.

PI3K, but not MAPK, participates in LN-2–enhanced myelin membrane sheet formation in oligodendrocytes in vitro. Previous findings had suggested that PI3K is involved in the regulation of actin cytoskeleton organization during integrin-mediated cell spreading (Seger et al., 2001). We show that PI3K inhibitors at concentrations (0.01 μM wortmannin and 0.5 μM LY294002) that do not affect cell viability prevent the formation of the LN-2–induced giant lamellae characteristic of oligodendrocytes, but do not change the number of $O1^+$cells. One reason why PI3K inhibitors might not affect cell survival on LN-2 is because LN-2 may switch in survival signaling, from PI3K to MAPK pathway in mature oligodendrocytes (Colognato et al., 2002).

Our results are supported by previous data showing that TSP-1 influences the migration (Scott-Drew and ffrench-Constant, 1997) and TN-C promotes proliferation (Garcion et al., 2001), but not differentiation through αvβ1 and αvβ3, respectively, in oligodendrocytes. In our short-term culture system, this LN-2–enhanced myelin membrane formation was not related to cell survival. However, previous studies have reported that LN-2 can function as a survival cue for mature oligodendrocytes (Colognato et al., 2002), and we cannot rule out the possibility that LN-2 in long-term culture might support oligodendrocyte cell survival.

ILK plays a critical role in oligodendrocyte cell spreading

Here, we show ILK expression in the CNS in vivo at high levels in interfascicular oligodendrocytes, with a time course that parallels myelination (Domercq et al., 1999). Because LN-2 is expressed on axons at the time of myelination (Powell et al., 1998), ILK may play an important role in LN-2–induced CNS myelination. Also, in the SN of the PNS, ILK was most prominent in Schwann cell cytoplasm, especially at and near nodes of Ranvier. Consistent with the in vivo data, we find that ILK is enriched in FAs in oligodendrocytes in vitro. Recently, ILK-deficient mice have been reported to die at the peri-implantation stage because of abnormal accumulation of actin at sites of integrin attachment at the basement membrane zone, and ILK-deficient fibroblasts show impaired cell spreading and delayed formation of FAs (Sakai et al., 2003). This implies a role for ILK in regulation of the actin cytoskeleton, which might be implicated in oligodendrocyte cell spreading. Furthermore, paxillin is important in regulation of the actin cytoskeleton in Schwann cells through integrin β1 (Taylor et al., 2003) and ILK colocalizes with paxillin in FAs (Nikolopoulos and Turner, 2001). We found that ILK is colocalized with integrin β1 and is associated with paxillin in FAs of differentiated oligodendrocytes on LN-2.

We also show that LN-2 stimulates ILK activity in oligodendrocytes and that the inhibition of ILK by DN-ILK blocks myelin membrane formation induced by LN-2. The interaction of the kinase domain of ILK with integrin β1, paxillin and PKB/AKT suggests that integrin β1, paxillin and PKB/AKT might be important regulators of the ILK-mediated signaling pathway for LN-2–induced oligodendrocyte cell spreading. Another possible mechanism through which ILK might influence oligodendrocyte cell spreading is suggested by the multidomain structure and FA localization of ILK, which imply that ILK might function as a scaffolding protein mediating multiple protein–protein interactions (Tu et al., 2001).

A distinction between hypomyelination and dysmyelination

Maturation of oligodendrocytes is a complex process that we have divided, in an attempt to unravel a temporal series of molecular control mechanisms, into arbitrary "stages", which include cell spreading, axonal ensheathment, and myelin compaction. We have shown that the *dy/dy* mouse has a reduced number of mature oligodendroglial cells and features hypomyelination and dysmyelination in several CNS tracts. ILK appears to be involved in the LN-2/integrin signaling that promotes the early maturational events of cell spreading and process formation. Hypomyelination is an expected consequence, but the basis for the dysmyelination component of the *dy/dy* phenotype remains to be elucidated. Many additional genes are also involved in oligodendrocyte maturation. Among them, the nonreceptor-type tyrosine kinase Fyn, a member of the src family, has been identified as a signaling molecule downstream of L-MAG (Umemori et al., 1994). Analysis of Fyn−/−, MAG−/−, and Fyn/MAG double knockout mice indicates that Fyn is involved in oligodendrocyte membrane and process formation, and MAG

in the formation of compact CNS myelin (Biffiger et al., 2000). There may be direct or indirect interactions of the ILK–LN-2–integrin components and the related FA proteins with Fyn, MAG, and additional molecular mediators.

Materials and methods

Animals

Homozygous 129/ReJ *dy/dy* mice and control littermates 5 wk old were purchased from The Jackson Laboratory. Dystrophic mice were distinguished from their littermates at 2–3 wk old, when they began to exhibit hindleg weakness. The +/+ and +/*dy* littermates were pooled as controls.

Reagents

LN-2, TN-C, and laminin-α2 chain (M-chain) antibody were obtained from CHEMICON International Inc.; PLO was obtained from Sigma-Aldrich; TSP-1 and ICN were obtained from Biomedicals; purified BSA was obtained from New England Biolabs, Inc.; wortmannin and LY294002 (PI3 K inhibitors) were obtained from Calbiochem; mAbs against A2B5, O4, and O1 were obtained from American Type Culture Collection; monoclonal and polyclonal anti-ILK and monoclonal anti–integrin β1, antipaxillin, and anti–β-tubulin antibodies and MBP were obtained from Upstate Biotechnology; antibody against MBP SMI99 was obtained from Sternberger Monoclonals; polyclonal antibodies against phospho-AKT ser473, AKT, phospho–GSK-3 ser9, and U0126 (MAPK inhibitor) were obtained from Cell Signaling; monoclonal CC1 antibody was obtained from Oncogene Research Products; secondary antibodies were obtained from Jackson ImmunoResearch Laboratories; Alamar blue assay kit was obtained from Treck Diagnostics; and the Live/Dead viability/Cytotoxicity assay kit was obtained from Molecular Probes.

Primary oligodendrocyte cultures

Primary cultures of OPCs were prepared from the cerebral hemispheres of 2-d-old Sprague-Dawley rats as described previously (Vartanian et al., 1997). Purified OPCs were plated on PLO-coated 60-mm dishes and incubated in the presence of 10 ng/ml PDGF and basic FGF for 3 d. To produce differentiated oligodendrocytes, cells were plated on different ECM substrates after trypsinization for 8–10 min and incubated in serum-free media with N_2 supplement (N_2) for another 3 d. Various ECMs, 10 μg/ml BSA, 1 μg/ml LN-2, 15 μg/ml TSP-1, and 3 μg/ml TN-C were incubated in PLO-coated 24-well dishes at 37°C for 1 h and washed three times with PBS.

Immunofluorescence microscopy

Immunofluorescence staining for A2B5, O4, or O1 was performed as described previously (Park et al., 2001). For the staining of FA proteins such as ILK, integrin β1, or paxillin, cells plated on LN-2 were extracted with 0.5% Triton-X 100 buffer before fixation. ONs from rats and control and *dy/dy* mice were dissected and immediately fixed in ice cold 4% PFA in 0.1 M phosphate buffer, pH 7.2, for 30 min. Fixed tissue was transferred to ice cold 20% sucrose (wt/vol) in 0.1 M phosphate buffer until equilibrated. Immunofluorescence staining was performed as described previously (Rasband et al., 1999). Immunofluorescent images were obtained with an objective (model Eclipse 660; Nikon) on 35-mm color film (ASA 400; Kodak), and digitized with a slide scanner or on an Axioskop 2 (Carl Zeiss MicroImaging, Inc.) fitted with a digital camera (model ORCA-ER; Hamamatsu).

Immunoblot

Primary cells were lysed in NP-40 lysis buffer (1% NP-40, 150 mM NaCl, 0.25% deoxycholate, 1 mM EGTA, 1 mM NaF, 50 mM Tris-HCl, 1 mM PMSF, and 2 mM sodium orthovanadate). For immunoblot analysis, cells were lysed in SDS sample buffer, boiled and subjected to SDS-PAGE followed by immunoblot. Incubation with primary antibodies was performed overnight at 4°C. For detection, HRP-conjugated secondary antibodies were used (1:5,000), followed by ECL development (Amersham Biosciences). 5-wk *dy/dy* and control mice were killed by CO_2 inhalation; the forebrain and the SC were removed and tissue homogenates were prepared in the lysis buffer. Blots were detected by primary antibodies such as MBP (1:1,000), ILK (1:1,000), and β-tubulin (1:1,000).

Coimmunoprecipitation

Lysates were prepared in serum-free media with N_2 for 30 min from either OPCs that had been incubated on different ECMs such as BSA and LN-2 or OPCs in suspension after trypsinization. Lysates prepared in NP-40 lysis buffer were incubated with antipaxillin antibody and protein G–agarose overnight at 4°C. After washing and boiling the beads, immunoprecipitates in SDS sample buffer were separated by electrophoresis on 10% SDS-PAGE, transferred to membranes, and probed with anti-ILK or paxillin antibodies. Kinase assay for ILK activity was performed as described previously (Ishii et al., 2001).

Viability studies

Cell survival was quantified by two rapid biochemical assays, the Alamar blue and Live/Dead Cytotoxicity assays. The Alamar blue assay (AccuMed International) was performed as described previously (Back et al., 1999). The Live/Dead Cytotoxicity assay is based on use of two probes, calcein AM and ethidium homodimer.

Adenovirus transfection

In the adenovirus-mediated Tet-off inducible system, infection of cells grown on LN-2 for 3 d with the recombinant TRE-adenovirus containing the pcDNA encoding HA-tagged DN-AKT (kinase inactive) with adenoviral tetracycline (Tet)-controlled transactivator (tTA) induced the expression of DN-AKT, and tetracycline (Tet) turned off its expression. ILK plasmids were provided by Shoukat Dedhar (Jack Bell Research Centre, Vancouver, Canada).

We generated recombinant GFP-adenovirus containing the pcDNA encoding either ILK or V5-His tagged-DN-ILK (kinase inactive). Cells that expressed GFP were assumed to be expressing the protein of interest. OPCs were plated on LN-2 and incubated with 10 or 20 MOI GFP-vector or GFP-DN-ILK in serum-free media with N_2 for 3 d. The infection rate of recombinant adenovirus GFP-ILK and GFP-DN-ILK was determined by the MOI that was expressed as the number of plaque forming units per cell.

Immunohistochemical staining

Mice were perfused with 4% PFA and held overnight in the same fixative. Segments of brain were embedded in paraffin and sectioned at 6 μm. The total cell concentration was counted in sections stained with H&E. Mature oligodendrocytes in the CC were identified in 6 μm paraffin sections incubated at 4°C overnight with CC1 (1:5). CC1 immunoreactivity was detected with the ABC Elite Kit for mouse (Vector Laboratories) with DAB substrate.

EM

Mice were anesthetized with CO_2 gas and perfused transcardially with 0.9% NaCl, followed by 2% PFA and 2.5% glutaraldehyde in 0.1 M cacodylate buffer, pH 7.4. Brain, ON, and cervical SC were then removed, trimmed, and held overnight in the same fixative. Tissue blocks were washed in 0.1 M cacodylate buffer, pH 7.4, and incubated for 1.5 h in 1% osmium tetroxide/1.5% potassium ferrocyanide, washed in H_2O, followed by maleate buffer, pH 5.2, and incubated for 1 h in 1% uranyl acetate in maleate buffer, pH 5.1. Blocks were washed in maleate buffer, dehydrated in graded ethanols, followed by propylene oxide, and embedded in TAAB Epon. Sections for light microscopy were cut at 0.5 μm and stained with alkaline toluidine blue. Ultrathin sections for EM were stained with uranyl acetate and lead citrate, and examined with a transmission electron microscope (model 1200EX; JEOL).

We thank Pieter Dikkes for technical assistance, and Jacob A. Sloane and N. Abimbola Sunmonu for their helpful comments with the manuscript.

This work was supported by grants from the National Institute of Neurologic Disorders and Stroke, R01 NS044916 to M.N. Rasband and R01 NS42317, K02 NS02028, and P01 NS38475 to T. Vartanian.

Submitted: 29 April 2003
Accepted: 8 September 2003

References

Back, S.A., R. Khan, X. Gan, P.A. Rosenberg, and J.J. Volpe. 1999. A new Alamar blue viability assay to rapidly quantify oligodendrocyte death. *J. Neurosci. Methods.* 91:47–54.

Biffiger, K., S. Bartsch, D. Montag, A. Aguzzi, M. Schachner, and U. Bartsch. 2000. Severe hypomyelination of the murine CNS in the absence of myelin-associated glycoprotein and fyn tyrosine kinase. *J. Neurosci.* 20:7430–7437.

Bjartmar, C., C. Hildebrand, and K. Loinder. 1994. Morphological heterogeneity of rat oligodendrocytes: electron microscopic studies on serial sections. *Glia.* 11:235–244.

Bradley, W.G., and E. Jaros. 1979. Involvement of peripheral and central nerves in

murine dystrophy. *Ann NY Acad Sci.* 317:132–142.

Buttery, P.C., and C. ffrench-Constant. 1999. Laminin-2/integrin interactions enhance myelin membrane formation by oligodendrocytes. *Mol. Cell. Neurosci.* 14:199–212.

Colognato, H., W.V. Baron, V. Avellana-Adalid, J.B. Relvas, A. Baron-Van Evercooren, and E. Georges-Labouesse, and C. ffrench-Constant. 2002. CNS integrins switch growth factor signaling to promote target-dependent survival. *Nat. Cell Biol.* 41:883–841.

Dedhar, S. 2000. Cell-substrate interactions and signaling through ILK. *Curr. Opin. Cell Biol.* 12:250–256.

Delcommenne, M., C. Tan, V. Gray, L. Rue, J. Woodgett, and S. Dedhar. 1998. Phosphoinositide-3-OH kinase-dependent regulation of glycogen synthase kinase 3 and protein kinase B/AKT by the integrin-linked kinase. *Proc. Natl. Acad. Sci. USA.* 95:11211–11216.

Domercq, M., M.V. Sanchez-Gomez, P. Areso, and C. Matute. 1999. Expression of glutamate transporters in rat optic nerve oligodendrocytes. *Eur. J. Neurosci.* 11:2226–2236.

Farina, L., L. Morandi, I. Milanesi, E. Ciceri, M. Mora, I. Moroni, C. Pantaleoni, and M. Savoiardo. 1998. Congenital muscular dystrophy with merosin deficiency: MRI findings in five patients. *Neuroradiology.* 40:807–811.

Feltri, M.L., D. Graus Porta, S.C. Previtali, A. Nodari, B. Migliavacca, A. Cassetti, A. Littlewood-Evans, L.F. Reichardt, A. Messing, A. Quattrini, U. Mueller, and L. Wrabetz. 2002. Conditional disruption of beta 1 integrin in Schwann cells impedes interactions with axons. *J. Cell Biol.* 156:199–209.

Fuss, B., B. Mallon, T. Phan, C. Ohlemeyer, F. Kirchhoff, A. Nishiyama, and W.B. Macklin. 2000. Purification and analysis of in vivo-differentiated oligodendrocytes expressing the green fluorescent protein. *Dev. Biol.* 218:259–274.

Garcion, E., A. Faissner, and C. ffrench-Constant. 2001. Knockout mice reveal a contribution of the extracellular matrix molecule tenascin-C to neural precursor proliferation and migration. *Development.* 128:2485–2496.

Guo, L.T., X.U. Zhang, W. Kuang, H. Xu, A. Liu, J.T. Vilquin, Y. Miyagoe-Suzuki, S. Takeda, M.A. Ruegg, U.M. Wewer, and E. Engvall. 2003. Laminin alpha2 deficiency and muscular dystrophy; genotype-phenotype correlation in mutant mice. *Neuromuscul. Disord.* 13:207–215.

Hildebrand, C., S. Remahl, H. Persson, and C. Bjartmar. 1993. Myelinated nerve fibres in the CNS. *Prog. Neurobiol.* 40:319–384.

Ishii, T., E. Satoh, and M. Nishimura. 2001. Integrin-linked kinase controls neurite outgrowth in N1E-115 neuroblastoma cells. *J. Biol. Chem.* 276: 42994–43003.

Kitamura, T., W. Ogawa, H. Sakaue, Y. Hino, S. Kuroda, M. Takata, M. Matsumoto, T. Maeda, H. Konishi, U. Kikkawa, and M. Kasuga. 1998. Requirement for activation of the serine-threonine kinase Akt (protein kinase B) in insulin stimulation of protein synthesis but not of glucose transport. *Mol. Cell. Biol.* 18:3708–3717.

Li, F., Y. Zhang, and C. Wu. 1999. Integrin-linked kinase is localized to cell-matrix focal adhesions but not cell-cell adhesion sites and the focal adhesion localization of integrin-linked kinase is regulated by the PINCH-binding ANK repeats. *J. Cell Sci.* 112:4589–4599.

Mackinnon, A.C., H. Qadota, K.R. Norman, D.G. Moerman, and B.D. Williams. 2002. C. elegans PAT-4/ILK functions as an adaptor protein within integrin adhesion complexes. *Curr. Biol.* 12:787–797.

Matsumura, K., H. Yamada, F. Saito, Y. Sunada, and T. Shimizu. 1997. Peripheral nerve involvement in merosin-deficient congenital muscular dystrophy and *dy* mouse. *Neuromuscul. Disord.* 7:7–12.

Morandi, L., C. Di Blasi, L. Farina, L. Sorokin, G. Uziel, G. Azan, A. Pini, A. Toscano, M. Lanfossi, S. Galbiati, et al. 1999. Clinical correlations in 16 patients with total or partial laminin alpha2 deficiency characterized using antibodies against 2 fragments of the protein. *Arch. Neurol.* 56:209–215.

Nikolopoulos, S.N., and C.E. Turner. 2001. Integrin-linked kinase (ILK) binding to paxillin LD1 motif regulates ILK localization to focal adhesions. *J. Biol. Chem.* 276:23499–23505.

Park, S.K., R. Miller, I. Krane, and T. Vartanian. 2001. The erbB2 gene is required for the development of terminally differentiated spinal cord oligodendrocytes. *J. Cell Biol.* 154:1245–1258.

Persad, S., S. Attwell, V. Gray, M. Delcommenne, A. Troussard, J. Sanghera, and S. Dedhar. 2000. Inhibition of integrin-linked kinase (ILK) suppresses activation of protein kinase B/Akt and induces cell cycle arrest and apoptosis of PTEN-mutant prostate cancer cells. *Proc. Natl. Acad. Sci. USA.* 97:3207–3212.

Powell, S.K., C.C. Williams, M. Nomizu, Y. Yamada, and H.K. Kleinman. 1998. Laminin-like proteins are differentially regulated during cerebellar development and stimulate granule cell neurite outgrowth in vitro. *J. Neurosci. Res.* 54:233–247.

Rasband, M.N., E. Peles, J.S. Trimmer, S.R. Levinson, S.E. Lux, and P. Shrager. 1999. Dependence of nodal sodium channel clustering on paranodal axoglial contact in the developing CNS. *J. Neurosci.* 19:7516–7528.

Sakai, T., S. Li, D. Docheva, C. Grashoff, K. Sakai, G. Kostka, A. Braun, A. Pfeifer, P.D. Yurchenco, and R. Fassler. 2003. Integrin-linked kinase (ILK) is required for polarizing the epiblast, cell adhesion, and controlling actin accumulation. *Genes Dev.* 17:926–940.

Schwab, M.E., and L. Schnell. 1989. Region-specific appearance of myelin constituents in the developing rat spinal cord. *J. Neurocytol.* 18:161–169.

Scott-Drew, S., and C. ffrench-Constant. 1997. Expression and function of thrombospondin-1 in myelinating glial cells of the central nervous system. *J. Neurosci. Res.* 50:202–214.

Seger, D., R. Seger, and S. Shaltiel. 2001. The CK2 phosphorylation of vitronectin. Promotion of cell adhesion via the alpha(v)beta 3-phosphatidylinositol 3-kinase pathway. *J. Biol. Chem.* 276:16998–17006.

Sperber, B.R., E.A. Boyle-Walsh, M.J. Engleka, P. Gadue, A.C. Peterson, P.L. Stein, S.S. Scherer, and F.A. McMorris. 2001. A unique role for Fyn in CNS myelination. 2001. *J. Neurosci.* 21:2039–2047.

Taylor, A.R., S.E. Geden, and C. Fernandez-Valle. 2003. Formation of a beta1 integrin signaling complex in Schwann cells is independent of rho. *Glia.* 41: 94–104.

Troussard, A.A., N.M. Mawji, C. Ong, A. Mui, R. St-Arnaud, and S. Dedhar. 2003. Conditional knock-out of integrin-linked kinase demonstrates an essential role in protein kinase B/Akt activation. *J. Biol. Chem.* 278:22374–22378.

Tsuji, S., and H. Matsushita. 1985. Evidence on hypomyelination of central nervous system in murine muscular dystrophy. *J. Neurol. Sci.* 68:175–184.

Tu, Y., Y. Huang, Y. Zhang, Y. Hua, and C. Wu. 2001. A new focal adhesion protein that interacts with integrin-linked kinase and regulates cell adhesion and spreading. *J. Cell Biol.* 153:585–598.

Turner, C.E. 2000. Paxillin and focal adhesion signalling. *Nat. Cell Biol.* 2:E231–E236.

Umemori, H., S. Sato, T. Yagi, S. Aizawa, and T. Yamamoto. 1994. Initial events of myelination involve Fyn tyrosine kinase signalling. *Nature.* 367:572–576.

Vartanian, T., A. Goodearl, A. Viehover, and G. Fischbach. 1997. Axonal neuregulin signals cells of the oligodendrocyte lineage through activation of HER4 and Schwann cells through HER2 and HER3. *J. Cell Biol.* 137:211–220.

Wu, C., and S. Dedhar. 2001. Integrin-linked kinase (ILK) and its interactors: a new paradigm for the coupling of extracellular matrix to actin cytoskeleton and signaling complexes. *J. Cell Biol.* 155:505–510.

Zervas, C.G., S.L. Gregory, and N.H. Brown. 2001. *Drosophila* integrin-linked kinase is required at sites of integrin adhesion to link the cytoskeleton to the plasma membrane. *J. Cell Biol.* 152:1007–1018.